

Electropolymerized durable coatings deposited onto Pt-electrode as corrosion inhibitor for mild steel

Ghada M. Abd El-Hafeez, Mohamed M. El-Rabeie, Ahlam F. Gaber & Zeinab R. Farag

To cite this article: Ghada M. Abd El-Hafeez, Mohamed M. El-Rabeie, Ahlam F. Gaber & Zeinab R. Farag (2021): Electropolymerized durable coatings deposited onto Pt-electrode as corrosion inhibitor for mild steel, Journal of Adhesion Science and Technology, DOI: [10.1080/01694243.2021.1963602](https://doi.org/10.1080/01694243.2021.1963602)

To link to this article: <https://doi.org/10.1080/01694243.2021.1963602>



Published online: 16 Aug 2021.



Submit your article to this journal [↗](#)



View related articles [↗](#)



View Crossmark data [↗](#)



Electropolymerized durable coatings deposited onto Pt-electrode as corrosion inhibitor for mild steel

Ghada M. Abd El-Hafeez, Mohamed M. El-Rabeie, Ahlam F. Gaber and Zeinab R. Farag 

Faculty of Science, Chemistry Department, Fayoum University, Fayoum, Egypt

ABSTRACT

Electropolymerization and deposition of poly(salicylic acid-co-N-methylaniline) copolymer, poly(SA-co-NMA) onto platinum electrode was studied using cyclic voltammetry in an acidic medium under inert conditions at various reaction factors. The mechanism of the electropolymerization reaction was proposed and the apparent activation energy (E_{app}) was determined. The deposited polymer film was characterized using different spectral tools such as UV spectroscopy, IR, ^1H NMR, X-ray, thermogravimetric analysis (TGA) and scanning electron microscopic (SEM) analysis, the spectral data for poly(salicylic acid) PSA and poly(N-methylaniline) PNMA were also given for comparison. The electropolymerized copolymer was collected from the Pt-surface then it has been investigated as a corrosion inhibitor. An open circuit potential method (OCP), electrochemical impedance spectroscopy (EIS) measurements and polarization techniques were used to study the application and the efficiency of the deposited copolymer film as corrosion inhibitor for mild steel in an acidic environment $\text{pH} = 2$.

ARTICLE HISTORY

Received 24 April 2021

Revised 12 July 2021

Accepted 29 July 2021

KEYWORDS

Electropolymerization; cyclic voltammograms; copolymer; polymer coatings; Kinetics; mild steel; corrosion inhibition

1. Introduction

Electroactive conducting polymers have a wide variety of applications in electronics and electro chemicals like sensors, photovoltaic cells, rechargeable batteries and corrosion protection [1–6]. The typical method is used to synthesize an electro-conductive polymer through electrochemical polymerization due its simplicity and reproducibility [7]. The electrochemical polymerization of monomers and their derivatives can be performed by various techniques such as potential sweep, potential step, potentiostatic and galvanostatic methods [8–11]. There are many factors that control the applications and properties of the electrodeposited polymer films, these factors include the nature and concentration of monomer adding to the effect of temperature, solvent as well as pH and voltammetric potential [12–14].

In electrochemical polymerization, a variety of reactions take place to produce the desired polymer film *via* oxidation of the monomer which forms free radicals that are adsorbed on the electrode surface. The deposited polymer is characterized by

its high purity in addition to its inherent physical properties to semi-conductors and metals as well as retaining the mechanical properties of conventional polymers [15].

Among the well-known conductive polymers which can be electrochemically deposited as films on metal or semiconductors electrodes are poly(aniline) PANI and its derivatives [16], poly(diphenylamine) and poly(aminoquinones) [17–21]. PANI can be polymerized by oxidative polymerization in aqueous acid [21] using various techniques such as electrodeposition, template synthesis, seeding and interfacial polymerization [22–26]. Other different polymers were used such as poly(vinyl alcohol) [27], poly(methacrylic acid) in the presence of iodide ions [28]

Phenols are another type of conducting polymers that can be electropolymerized in both aqueous and non-aqueous solutions by oxidation to form adherent thin polymeric films of low permeability and low water mobility [29] Phenol and various *p*-substituted phenols (namely, *p*-cresol, hydroquinone, *p*-chlorophenol, *p*-bromophenol, *p*-nitrophenol, *p*-aminophenol, *p*-hydroxy-[27,30,31]. Aljeaban et al. recently studied the mitigation of steel corrosion using decorated polymers with functional motifs [32] Phenol polymers have many biological and chemical applications such as antibiotic, antioxidant activity and antifouling actions due to their diverse structures. Plants Polyphenols have been used as an alternative green corrosion inhibitor for mild steel in acidic media [33], Thiphenol and thiophenol derivatives were also studied [34].

Steel has a number of desired properties, such as hardness, ductility, weldability and durability, so it is one of the most widely used metals, which is applied in many infrastructures. However, corrosion is still the severe problem, which causes degradation and affects the safety and service life of steel structures [35]. The deposition of electropolymerized polymer films on the surface of a metallic electrode is a common protective technique in electrochemistry. Traditional polymer coatings are one of the prevailing corrosion inhibitors that act as physical and an electronic barrier due to their good surface coverage adding to their high resistance, excellent mechanical properties and are also ecofriendly [36–41]. Epoxy coatings with the incorporation of poly(pyrrole-graphene) nanocomposites are recently used for steel protection [42,43]. Different polymers have been studied as corrosion inhibitors in acid medium of HCl such as of poly(aniline-co-metanic acid) and poly(styrene sulfonic acid) doped polyaniline [44,45], A copolymer of (aniline-co-*o*-toluidine) and (*o*-bromophenol-co-*N*-methylaniline) coatings have been reported [46,47].

In this work poly(SA-co-NMA) was electrodeposited on Pt-electrode the deposited polymer film was then characterized and a proposed mechanism for the polymerization reaction was suggested. Optimization of the parameters affecting the electropolymerization reaction has been studied. The deposited film which formed at the optimum conditions is collected by scratching from the Pt-electrode and then it was investigated as a corrosion inhibitor for mild steel in acidic solutions (pH = 2).

2. Experimental

2.1. Materials

N-methylaniline (NMA) and salicylic acid (SA) and were obtained from (Merck Schuchardt, Germany), sulfuric acid, ethanol and acetone from El-Nasr Company for

Table 1. Chemical composition of the mild steel electrode.

Element	C	Si	Mn	S	P	Cu	Cr	Ni	Mo	Al	Fe
Analysis	0.34	0.26	0.93	0.02	0.04	0.01	0.01	0.02	–	0.01	Balance

Intermediate Chemicals NCIC, Egypt. The used chemicals were of A.R. grade and used as received. Solutions were prepared using DDW and acidic buffer of pH = 2.

2.2. Electropolymerization cell

Electropolymerization reaction was performed using the potentiodynamic technique. Perspex trough cell was used its inner dimensions are 2.5 cm width, 3 cm height and 8 cm length.

A Pt-sheets (dimensions = 0.5 cm width and 1 cm length) were used as working electrode (WE) and the auxiliary (counter) electrode (CE). The reference electrode is a saturated calomel electrode (SCE), its potential value is 0.242 V. The electrode potential is given relative to SCE. A pure carbon steel electrode and its composition is given in Table 1.

2.3. Preparation of the polymer solution used for corrosion measurements

The potentiodynamic cyclic voltammetry measurements were carried out using an electrochemical cell during the electropolymerization process. The cell was filled with the supporting electrolyte (aqueous H₂SO₄ solution), monomer and acetone (solvent). Then, CE and the WE were inserted into the cell. A U-shaped salt bridge (SB) was used to attach the reference electrode to the cell, and it is ended with Luggin–Harber probe fine capillary tip. SCE and WE were positioned very close to each other to minimize the over potential. A stream of pure N₂ gas bubbled for 3 min into the test solution in order to remove any dissolved gases before and during the measurements. Potentiostat/Galvanostat Wenking (PGS 95) was used to perform electrochemical experiments. ECT software was used to record I–E curves. The potential was linearly swept from the starting potential vs. (SCE) to the positive value with a given scan rate up to a specific anodic potential, then the potential was reversed to the starting cathodic potential with the same scan rate. A cleaned cell and freshly prepared solutions were used for each run, electrodes were washed thoroughly with ethanol, rinsed with DDW and then dried to remove any formed residuals in the reaction medium. The temperature was controlled using a circular water thermostat.

Poly(SA-co-NMA) was prepared from an aqueous solution containing 0.060 mol L⁻¹ of monomer, 0.2 mol L⁻¹ H₂SO₄ at 30 °C with scan rate 40 mVs⁻¹

The working electrode was a Pt-sheet with dimensions of 1 cm length and 0.5 cm width containing a 0.75 cm Pt-wire for electrical connection. The Pt-electrode was cleaned with ethanol, DDW and dried for each measurement.

The testing solution was prepared to be of weight 0.1g from polymer, with drops of ethanol to dissolve the polymer followed by the addition of 100 ml acidic solution (1 M H₂SO₄). Then this solution was used to prepare different concentrations (0 ppm, 20 ppm, 50 ppm and 100 ppm) of the polymer.

2.4. Open circuit potential measurements

The working electrode potential under open-circuit conditions was measured separately against the saturated calomel electrode (SCE) as reference electrode (Hg/Hg₂Cl₂/Cl-sat)]. The standard electrode potential, $E_o = 242$ mV was estimated versus the standard hydrogen electrode (SHE). A high impedance multimeter was used for open circuit potential measurements over a period of 1 h.

2.5. Electrochemical system

The VoltaLab 10PGZ100 'All-in-One' Potentiostat/Galvanostat was used to measure electrochemical impedance and polarization. The device was connected to an external IBM 1200 CPU computer. The voltamaster software was used to investigate the potentiodynamic polarization and electrochemical impedance spectroscopy (EIS). The experimental setup and procedure enabled the direct application of any above-mentioned techniques. Both linear polarization and Tafel techniques were used after each impedance experiment, which was always performed on open circuit potential.

2.5.1. Potentiodynamic polarization techniques

The corrosion rate is usually attained utilizing the methods of linear polarization and Tafel extrapolation. Potentiodynamic measurements were performed at 10 mV/s scan rate. The output current was plotted linearly against the potential and the slope of this potential current function at the corrosion potential (E_{corr}), denoted as the polarization resistance R_p , and used with the Tafel constants to determine the corrosion current density (i_{corr}). The linear polarization technique was very fast, making the measurements very useful in the applied potential, which was not far from the corrosion potential.

Thus, the sample surface was not significantly affected by the experiment and can often be used in other studies.

$$R_{\text{corr}} \equiv (\beta_a \beta_c) / 2.3(\beta_a + \beta_c) i_{\text{corr}} \quad (1)$$

where β_a and β_c are the anodic and cathodic Tafel slopes, respectively. After reaching the steady state, both R_{corr} and i_{corr} values were calculated directly [48]. In order to predict the inhibition efficiency, the following equation has been applied:

$$\eta \% = [(i - i_{\text{inh}}) / I] \times 100 \quad (2)$$

where i and i_{inh} are the corrosion current densities before and after the corrosion inhibition process.

2.5.2. Impedance measurements

The electrochemical impedance spectroscopy is an essential technique for investigating electrochemical and corrosion systems. The major feature of this technique is the employment of a purely electronic model (equivalent circuits [Figure 1](#)) to demonstrate the electrode/electrolyte interface under different conditions. An interface that

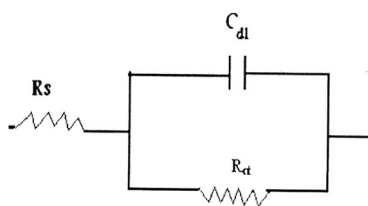


Figure 1. Equivalent circuit.

experiences an electrochemical reaction usually resembles an electronic circuit consisting of resistors, capacitors, and/or conductors. Hence, the electrochemical system can be described in terms of its equivalent circuit. According to the theory of an alternating current circuit, the impedance diagram obtained for a given electrochemical system can be related to one or more equivalent circuits.

The mathematical formulation to measure the electrode impedance (Z) is as follows:

$$Z = R_s + [R_{ct}/1 + (2\pi f R_{ct} C_{dl})^\alpha] \quad (3)$$

where R_s is the solution resistance, connected to a parallel combination of representing the charge transfer resistance R_{ct} at the electrode/electrolyte interface and C_{dl} , representing the double layer empirical parameter ($0 \leq \alpha \leq 1$) [49,50].

2.6. Characterization of the electrodeposited polymer

Chemical analyses were carried out at the micro-analytical center, Cairo University, Cairo, Egypt.

- UV spectra of the electrodeposited polymer were performed with (SHIMADZU M160 PC) spectrophotometer in the range of 200–400 nm at room temperature using ethanol (as reference and a solvent).
- FTIR – 340 Jasco spectrophotometer (Shimadzu, Japan) was used to record IR measurements using KBr disk technique.
- A Nuclear Magnetic Resonance spectrometer (Varian EM 360L, 60-MHz) was used for ^1H NMR measurements using Dimethylsulphoxide (DMSO) as solvent.
- Thermogravimetric analysis (TGA) was carried out using a thermal analyzer of the type DT-30 (SHIMADZU, Kyoto, Japan). The measurements were recorded from room temperature up to 600°C , at the rate of $20^\circ\text{C}/\text{min}$ and N_2 $50\text{ cm}^3/\text{min}$.
- Scanning electron microscopy (SEM) was achieved utilizing a JSM-T20 Electron Probe Micro analyzer (JEOL, Tokyo, Japan).
- The X-ray diffraction analysis (XRD) (Philips 1976 Model 1390, Netherlands) has been operated using Cu X-ray tube. The measurements were carried out at a scan speed: $8\text{ deg}/\text{min}$, 30 mA Current, 40 kV Voltage and 10 s preset time.

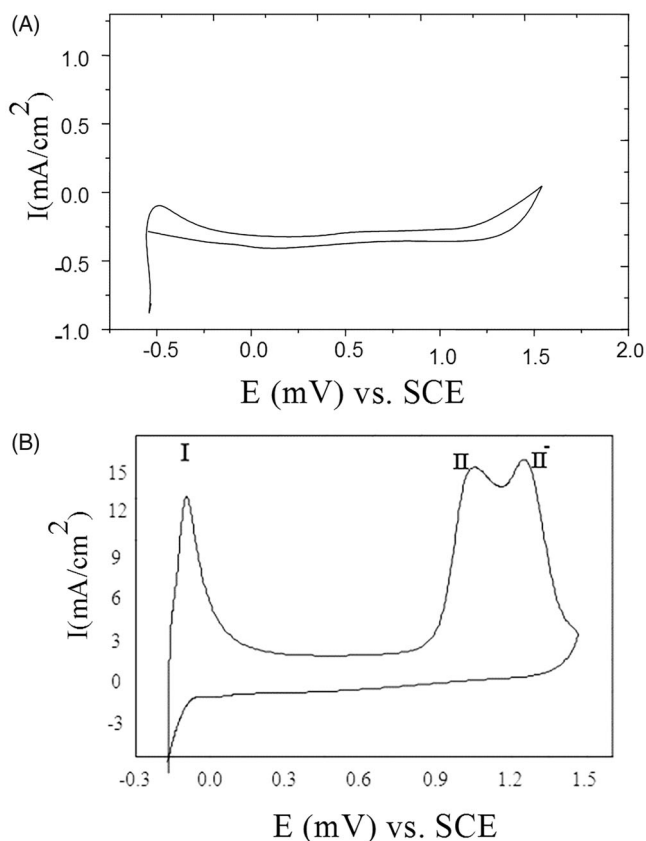


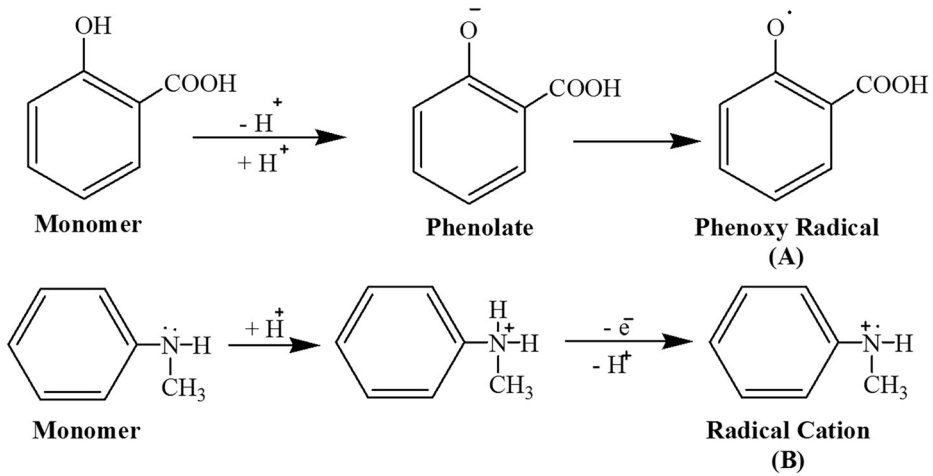
Figure 2. Cyclic voltammograms of solution containing 0.4 mol/L H_2SO_4 at 303 K with scan rate 40 mV/s. (A) Without, (B) With 0.05 mol/L monomer.

3. Results and discussion

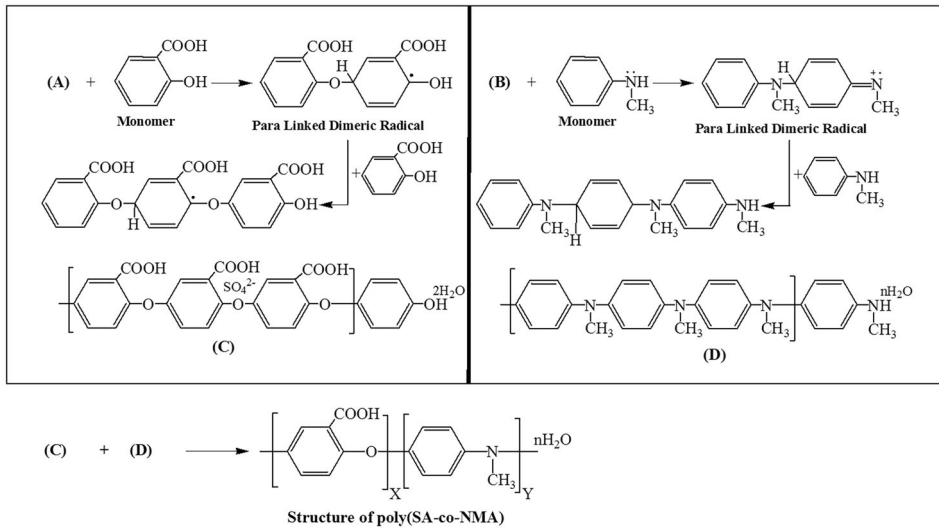
3.1. Electrodeposition of poly(SA-co-NMA) by cyclic voltammetry

Cyclic voltammetry of the polymerization of SA and NMA on Pt-electrode using 0.4 mol/L H_2SO_4 with a scan rate of 40 mV/s at 303 K was measured. The cyclic voltammogram was started from -500 to $+1500$ mV (vs.SCE) as shown in Figure 2(A,B). In absence of the monomer, an oxidation peak at -100 mV (vs. SCE) was observed as result of adsorption of hydrogen on Pt-electrode [51] (Figure 2(A)). While, the voltammogram in the presence of 0.05 mol/L of monomer it showed three progressively developed oxidation peaks (I, II and II') at ~ -100 , $\sim +1050$ and $\sim +1250$ mV(vs. SCE) respectively (c.f. Figure 2(B)). The first oxidation peak (I) was due to the reduction of hydrogen [51], while the second and the third peaks (II and II') were attributed to the adsorption of the phenoxy radical on Pt-electrode as a result of the oxidation of the monomer [52].

SA and NMA molecules react with the adsorbed radicals forming a para-linked dimeric radical *via* head-to-tail coupling producing an oligomer and a polyether polymer film composed of isolated aromatic rings without delocalization of π -electrons as represented later in Scheme 2. However, a brown polymeric film was deposited on the



Scheme 1. Initiation step of the polymerization reaction.



Scheme 2. Propagation step of the polymerization reaction.

surface of the Pt-electrode as soon as polymerization process is initiated. The potential difference between peak I and II' (the first oxidation peak and the third one) was $\approx +1350$ mV, which proved the absence of degradation products, this potential difference also indicated that the polymer film was deposited with high regularity, homogeneity and of a good adherence [53].

3.2. Electropolymerization mechanism

The anodic oxidative polymerization of poly(SA-co-NMA) was proceeded as follows:

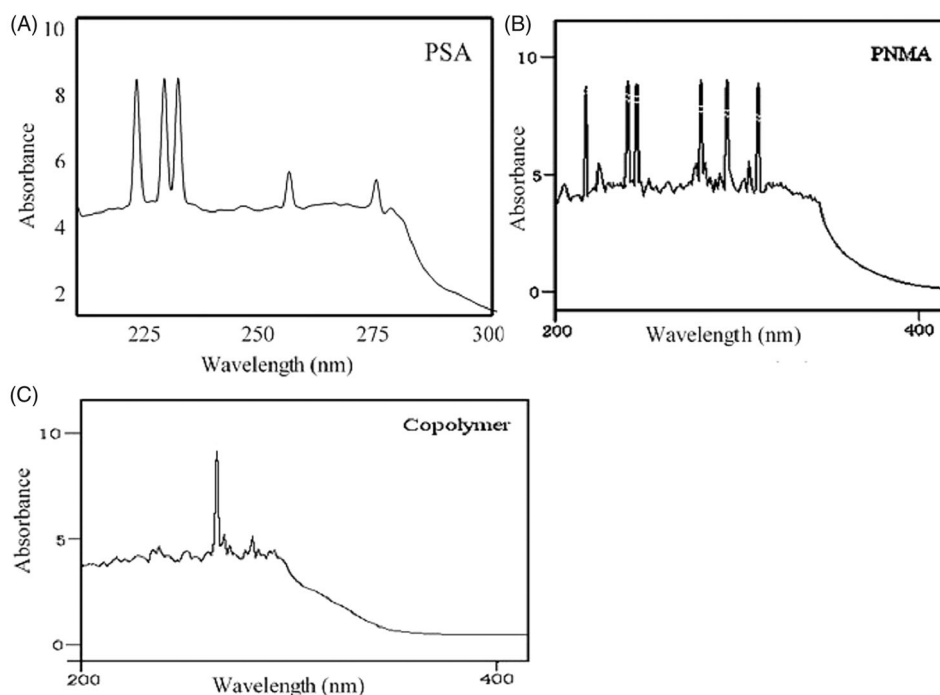


Figure 3. The UV-visible assignments of (A) PSA, (B) PNMA and (C) poly(SA-co-NMA).

3.2.1. Initiation

The initiation of the polymerization reaction is represented by [Scheme 1](#).

3.2.2. Propagation

[Scheme 2](#) represents the propagation step of the electropolymerization reaction of poly(SA-co-NMA).

3.2.3. Termination

By the finishing of the run.

3.3. Characterization of the deposited polymers

Due to the different possibilities of copolymer structures, the elemental analysis data became unuseful. The structure of the obtained copolymer was confirmed by UV-Visible, IR, $^1\text{H-NMR}$, TGA, XRD and SEM. The suggested structures of the obtained polymers were presented in [Scheme \(2\)](#).

3.3.1. The ultraviolet-visible (UV-Vis) spectra

The UV-Visible spectra of PSA, PNMA and poly(SA-co-NMA) are given in [Figure 3](#):

1. The absorption bands at $\lambda_{\text{max}} = 230, 270$ and 277nm that may be attributed to (E_2 -band) which corresponds to the transition of benzene ring and the other is β -band ($A_{1g}-B_{2u}$) as illustrated in [Figure 3\(A\)](#).

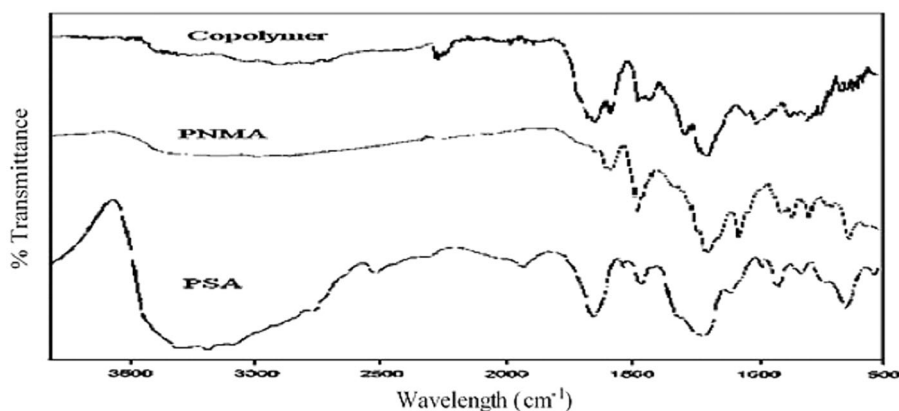


Figure 4. The infrared spectra of PSA and PNMA and poly(SA-co-NMA).

2. The absorption bands at $\lambda_{\max}=220, 243, 253, 290, 310$ and 325nm is due to the transition (E_2 -band) corresponds to a benzene ring and β -band ($A_{1g}-B_{2u}$), respectively, as shown in [Figure 3\(B\)](#).
3. Two absorption bands appeared at $\lambda_{\max} = 275$ and 290 nm in the case of poly(SA-co-NMA) due to the higher conjugation of the aromatic polymeric chains as represented in [Figure 3\(C\)](#).

3.3.2. Infrared (IR) spectroscopy

The infrared spectra of PSA, PNMA and poly(SA-co-NMA) are represented in [Figure 4](#). The infrared absorption bands are summarized in [Table 2](#).

3.3.3. ^1H NMR spectroscopic measurements

The ^1H NMR spectrum of PSA, PNMA and the prepared poly(SA-co-NMA) were represented in [Figure 5](#). The protons of multiplet signals of aromatic rings were appeared in the region from $\delta = 6.95 - 7.84\text{ ppm}$ for all polymers, for PNMA the aromatic signals of which are highly reduced due to their low intensity as a result of the presence of some quinonoid structures. The methyl group protons appeared at 1.25 ppm . The solvent protons appear as singlet, doublet and singlet signals in the range $2.95-3.6\text{ ppm}$, respectively [54]. A para-linked - disubstituted aromatic ring which could be part of an oligomeric structure in which a corresponding methyl group singlet is found at $\delta = 2.88\text{ ppm}$ [55]. The signals of -OH group were removed upon using a deuterated solvent.

3.3.4. Thermogravimetric analysis (TGA)

Thermogravimetric analysis (TGA) for the electrodeposited copolymer was investigated and represented in [Figure 6](#). The presence of water molecules and two acid molecules per repeated unit was confirmed by thermogravimetric analysis. There are four phases during the thermolysis of the prepared polymer samples:

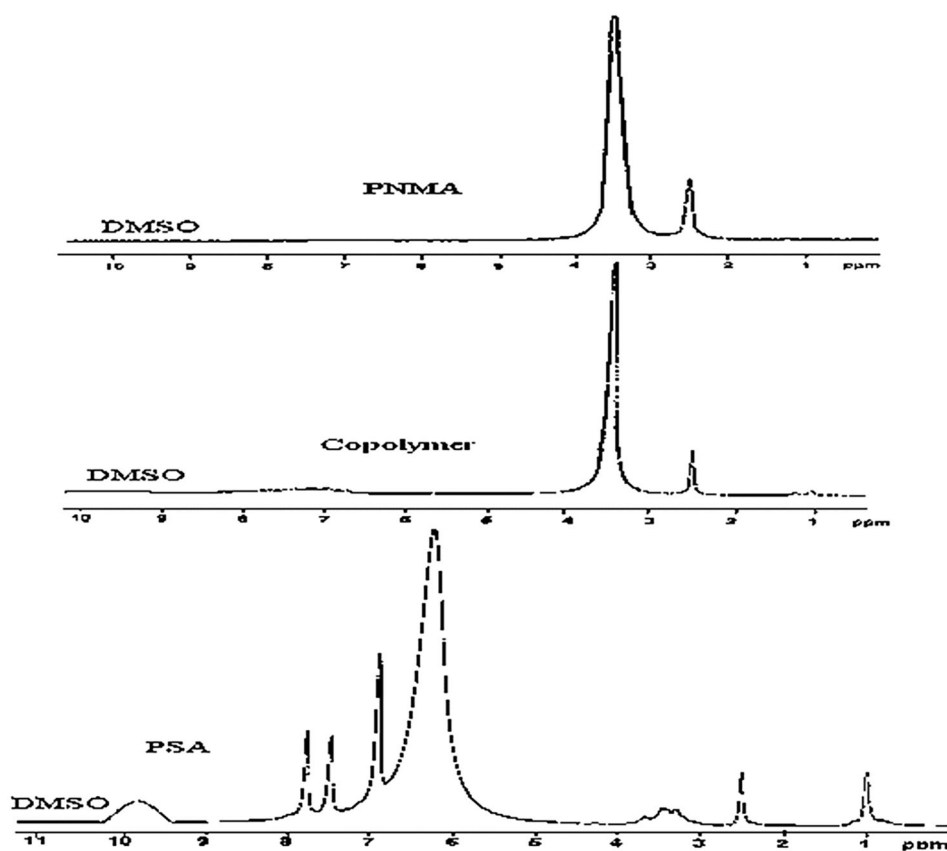
The first phase: the removal of water molecules started at 43.22°C up to 66.08°C .

The second phase: at $150-200^\circ\text{C}$ the bonded water molecules are thermally decomposed.

Table 2. Infrared absorption bands of PSA, PNMA and poly(SA-co-NMA).

Assignments	Wave number (cm ⁻¹)		
	PSA	PNMA	Copolymer
CH out of plane bending for 1,2 di-substituted benzene ring	580 ^s	665 ^m	680 ^s
	768 ^w	–	763 ^m
CH out of plane bending for 1, 2, 4 tri-substituted benzene ring.	869 ^m	815 ^m	886 ^s
Stretching vibration for C–O group.	–	1035 ^w	1024 ^w
Stretching for incorporation in the polymer sulfate group.	1218 ^b	–	1193 ^b
Stretching vibration of C=C in benzene ring	1456 ^s	–	1454 ^m
	1656 ^b	1619 ^w	1660 ^s
Stretching vibration for CH aromatic	2600 ^w	–	2597 ^b
	2876 ^w	–	2856 ^s
	–	–	2999 ^w
Stretching vibration intermolecular hydrogen solvated OH group or end group OH of polymeric chain.	–	3226 ^b	3233 ^b
	3496 ^b	–	3437 ^w

s: strong; w: weak; b: broad; m: medium.

**Figure 5.** The ¹H NMR spectra of PSA, PNMA and poly(SA-co-NMA).

The third phase: at the temperature range from 180 °C to 350 °C the decomposition of dopants present in the polymer structure

The fourth phase: the decomposition of the remaining part of the polymer is the last stage in the range from 385 °C to 600 °C.

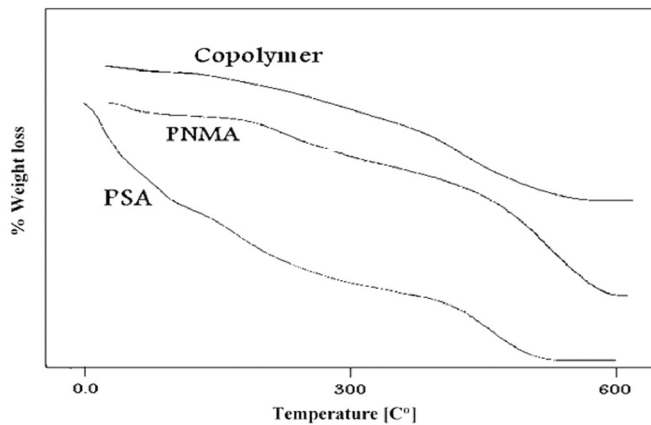


Figure 6. Thermogravimetric analysis of PSA, PNMA, poly(SA-co-NMA).

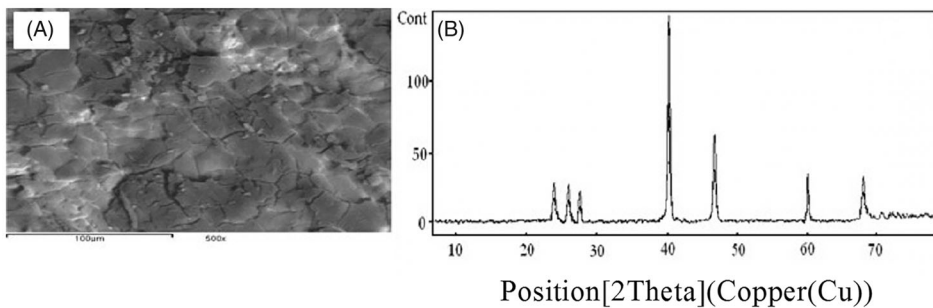


Figure 7. (A) The scanning electron microscope (SEM), (B) The X-ray diffraction (XRD) of poly(SA-co-NMA).

It was observed that the polymer backbone chains were decomposed at different temperatures depending on the polymer structure. In addition, the copolymerization of NMA and SA enhanced the thermal stability of the copolymer.

3.3.5. Surface analysis and X-ray diffraction (XRD)

The electrodeposited film of poly(SA-co-NMA) copolymer on Pt-electrode surface at the optimum conditions, was brown, homogeneous, smooth and have excellent adhesion properties. The surface morphology of the electrodeposited copolymer film was examined by scanning electron microscopy (SEM) and XRD.

SEM micrographs showed that the surface of the electrodeposited polymer film was smooth and lamellar as presented in Figure 7(A). The XRD pattern displayed in Figure 7(B) revealed surface crystallization of the prepared copolymer.

3.4. Open circuit potential measurements

Figure 8 represented the open circuit potential of mild steel in the presence of different concentrations of co-polymers such as salicylic acid and N-methylaniline (0, 20 ppm, 50 ppm and 100 ppm) over one hour in a naturally stagnant aerated acid solution (1 M

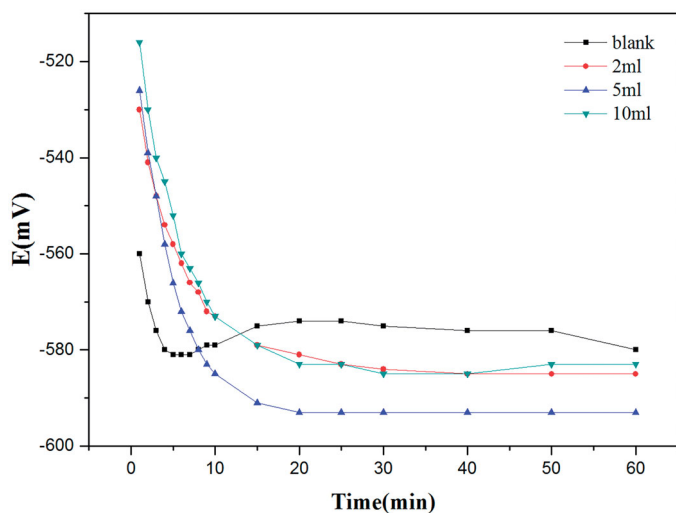


Figure 8. Variation of the open-circuit potential of mild steel alloy with time in stagnant naturally aerated aqueous acidic solution (1 M H_2SO_4) in the presence of different concentrations of poly(SA-co-NMA) at 25 °C.

H_2SO_4). The results showed that the presence of the polymer transfers the steady-state potentials to more negative values indicating the presence of a passive film.

3.5. Potentiodynamic polarization measurements

The electrochemical behavior of mild steel was evaluated with different concentrations of poly (SA-co-NMA) (blank, 20 ppm, 50 ppm, 100 ppm) in an acidic solution (1 M H_2SO_4) under polarization conditions. The linear polarization and Tafel extrapolation techniques were applied at scan rate 10mVs^{-1} . Figure 9 illustrated that the potentiodynamic polarization curves of different concentrations of poly(SA-co-NMA) after holding the mild steel electrode at the open circuit potential for 1 h in naturally aerated aqueous acidic solution (1 M H_2SO_4). The corrosion potential was evidently shifted negatively in the presence of different concentrations of the examined co-polymers. The co-polymer also reduced both anodic and cathodic branches. The tested co-polymer acts as a mixed inhibitor, that is, the studied co-polymer adsorbed both anodic and cathodic active sites on the metallic surface, blocking the active sites of the corrosion process, thus reducing the free metal surface area exposed to a corrosive medium.

The impact of the inhibitor relied on two factors: the electronic structure of both the inhibitor and the metal and the molecular structure of the inhibitor [56,57].

For the first factor, the inhibition efficiency will increase as the chain length of the side group increases due to the increase in the metal-covered surface area. The presence of a lone pair of electrons on the N and O atoms in the prepared polymer will assist in the adsorption on the metal surface. For the second factor, the presence of the d orbital in the iron metal in the alloy gives a high chance of adsorption. So that the

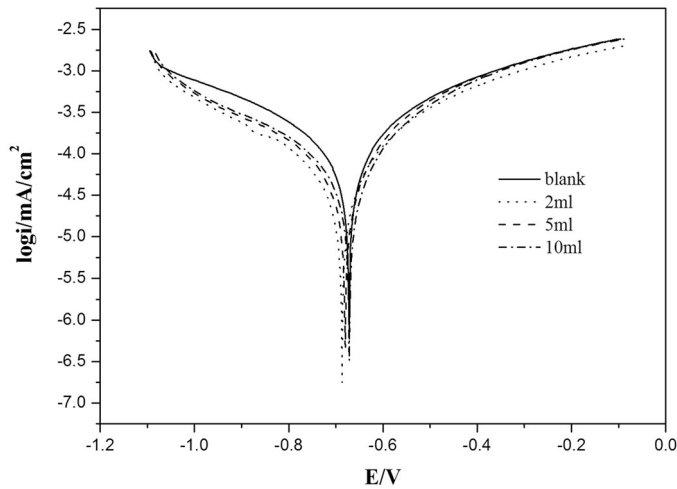


Figure 9. Potentiodynamic polarization curves of mild steel alloy in stagnant naturally aerated aqueous acidic solution (1 M H₂SO₄) in the absence and presence of different concentrations of poly(SA-co-NMA) at 25 °C.

Table 3. Potentiodynamic polarization parameter of steel after 1 h of electrode immersion in stagnant naturally aerated poly(SA-co-NMA) solution in naturally aerated aqueous acidic solution (1 M H₂SO₄) at 25 °C.

Concentration	E_{corr} / mV	R_p / Ω cm ²	i_{corr} / μ Acm ⁻²	β_a / mV	β_c / mV	Corrosion rate/ μ my ⁻¹	η %
Blank	-670.6	502	107.1	263.4	-345.1	1.33	0
20 ppm	-670.2	890	75.4	239.0	-373.2	0.94	42.0
50 ppm	-678.9	880	59.7	195.1	-307.1	0.74	44.3
100 ppm	-685.3	1040	33.7	154.1	-207.8	0.42	68.5

effect of inhibition of the prepared co-polymer is due to the adsorption on the mild steel alloy.

Table 3 illustrated the calculated values of corrosion parameters (Tafel slopes (β_a and β_c), corrosion current density (i_{corr}), corrosion potential (E_{corr}), corrosion rate of the prepared co-polymer film. The corrosion inhibition efficiency η was estimated at different concentrations of the prepared co-polymer according to:

$$\eta = [(i - i_{inh})/i] \times 100 \tag{2}$$

where i is the corrosion current density for the alloy in the absence of the inhibitor and i_{inh} is the value after adding a certain amount of inhibitor under the same conditions. Values of η in all cases are also listed in Table 3.

The corrosion current density and corrosion rate decreased with increasing polymer concentration, this indicated that the prepared polymer has good inhibitory properties.

3.6. The electrochemical impedance measurements

The impedance spectra were determined at the open circuit potential for mild steel in various concentrations of the co-polymers examined in a naturally aerated

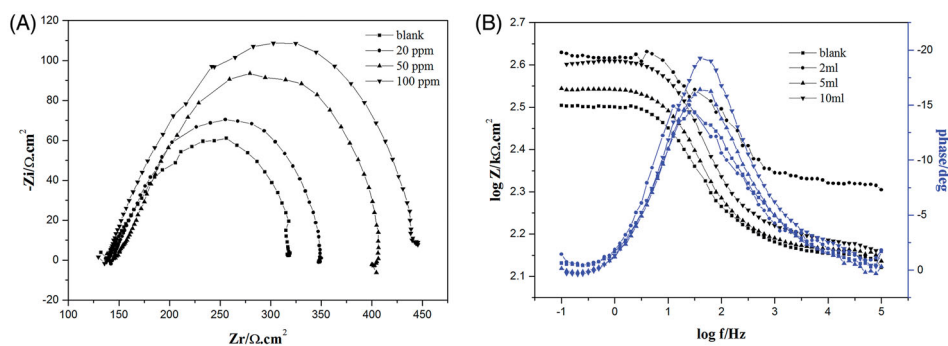


Figure 10. (A) Nyquist plot of mild steel alloy in stagnant naturally aerated aqueous acidic solution (1 M H₂SO₄) in the absence and presence of different concentrations of poly(SA-co-NMA) at 25 °C. (B) Bode plot of mild steel alloy in stagnant naturally aerated aqueous acidic solution (1 M H₂SO₄) in the absence and presence of different concentrations of poly(SA-co-NMA) at 25 °C.

Table 4. Equivalent circuit parameters for steel recorded after 1 h of electrode immersion in stagnant naturally aerated poly(SA-co-NMA) solution at steady state potential at 25 °C.

Concentration	$R_s / \Omega \text{ cm}^2$	$R_p / \Omega \text{ cm}^2$	$C_{dl} / \mu\text{Fcm}^{-2}$	$\eta \%$
blank	143.1	183.0	34.8	–
20 ppm	146.2	204.9	31.1	10.7
50 ppm	147.1	206.0	30.9	11.2
100 ppm	153.9	259.0	19.4	29.3

acidic solution (1 M H₂SO₄). The results obtained for the impedance measurements were depicted in Figure 10(A) (the Nyquist plot) and 10 b (Bode plot). The system response in the Nyquist complex plane (Figure 10(A)) consists of one semicircle.

The time constant or diameter of the semi-circle increases with increasing concentrations of the prepared co-polymer. Figure 10(B) showed that a single clear maximum phase exists for a mild steel electrode with an intermediate frequency. This constant appeared once as a well-defined capacitive loop at the intermediate frequency region in the Nyquist plot (Figure 10(A)). The intermediate time constant was attributed to the presence of a protective surface film [49,50].

Table 4 showed the equivalent circuit parameter for mild steel determined after 1 h of electrode immersion in stagnantly naturally aerated acidic aqueous solutions in the absence and presence of the prepared co-polymer at steady-state potential at 25 °C. It is clear that the R_{ct} increased with increasing the co-polymer concentration, and also C_{dl} decreased with the increase in the polymer concentration. The equivalent circuit parameters calculated from these data showed that the poly(SA-co-NMA) formed a passive layer on a mild steel surface.

3.7. Adsorption isotherm

To get information about the nature of the interaction between the prepared polymer and the electrode surface, various adsorption isotherms were examined. The data presentation showed that the adsorption process was according to the

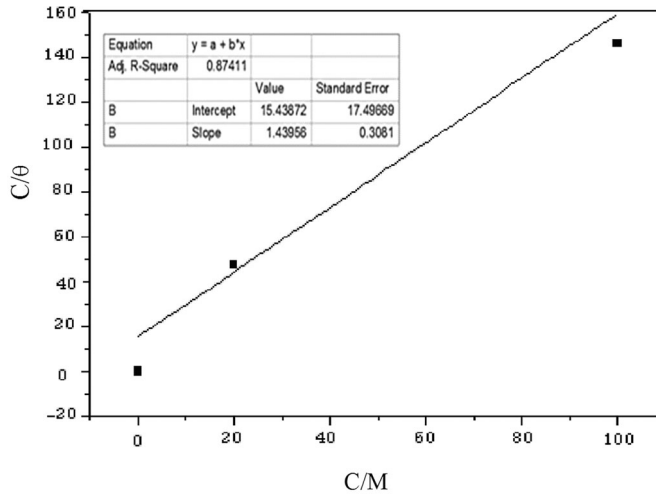


Figure 11. Langmuir isotherm plot for the adsorption of poly(SA-co-NMA) on mild steel alloy in stagnant naturally aerated aqueous acidic solutions (1 M H₂SO₄) at 25 °C.

Langmuir adsorption isotherm for the adsorption of a prepared co-polymer on mild steel in a naturally aerated aqueous stagnant acid solution (1 M H₂SO₄) at 25 °C. The data presented in Figure 11 are calculated following the mathematical formulation:

$$KC = \theta/1-\theta \quad (4)$$

where C is the concentration of the inhibitor, θ is the fractional surface coverage and K is the adsorption equilibrium constant related to the free energy of adsorption, ΔG_{ads} , as follows:

$$K = 1/C_{\text{solvent}} \exp(-\Delta G_{\text{ads}}/RT) \quad (5)$$

where C_{solvent} is the molar concentration of the solvent (H₂O = 55.5 mol dm⁻³), T is the absolute temperature and R is the universal gas constant (8.314 J mol⁻¹K⁻¹).

The Langmuir adsorption isotherm may be rearranged to get the following mathematical formulation:

$$C/\theta = 1/K + C \quad (6)$$

A linear relationship can be obtained where C is a slope and the value of the intercept is the reciprocal of K . The calculated values for the adsorption of the co-polymer prepared on a mild steel surface were -3.17 kJ/mol, which was less than -40 kJ/mol, indicating physical adsorption, and there is no chemical interaction between the inhibitor molecules and the alloy surface. The low and negative value of ΔG_{ads} indicated spontaneous adsorption of the co-polymer prepared on the mild steel surface [58].

Conclusion

A conducting polymer film was synthesized by electrochemical polymerization of salicylic acid SA and N-methylaniline NMA monomers. The formed polymer was deposited on Pt-electrode. The electrodeposited poly(SA-co-NMA) film was characterized and the kinetics of the polymerization reaction was investigated. The results show that the deposited polymer has excellent thermal properties with homogeneous, regular and smooth lamellar surface. The deposited polymer was collected from the Pt surface by scratching and investigated as a corrosion inhibitor. The corrosion behavior of mild steel samples using cyclic voltammetry electropolymerization technique of poly(SA-co-NMA) was then studied. The results showed that the deposited polymer films have higher thermal stability with the homogeneous and smooth lamellar surface. Also, the corrosion resistance of the coated mild steel samples increased with the increase in the polymer concentration as well as the corrosion protection efficiency.

Disclosure statement

No potential conflict of interest was reported by the author(s).

ORCID

Zeinab R. Farag  <http://orcid.org/0000-0003-4198-8417>

References

- [1] Cosnier S. Biomolecule immobilization on electrode surfaces by entrapment or attachment to electrochemically polymerized films. A review. *Biosens Bioelectron.* 1999;14(5): 443–456.
- [2] De Paoli M-A, Gazotti WA. Electrochemistry, polymers and opto-electronic devices: a combination with a future. *J Braz Chem Soc.* 2002;13(4):410–424. doi:<http://dx.doi.org/10.1590/S0103-50532002000400003>.
- [3] Fomo G, Waryo T, Feleni U, Baker P and Iwuoha E.. Electrochemical polymerization, , in *Functional Polymers*, edited by M. A. Jafar Mazumder, H. Sheardown and A. Al-Ahmed. Springer International Publishing, City. 2019), pp. 105.
- [4] Gupta G, Birbilis N, Cook AB, et al. Polyaniline-lignosulfonate/epoxy coating for corrosion protection of AA2024-T3. *Corros Sci.* 2013;67:256–267.
- [5] Islam R, Le Luu HT, Kuss S. Electrochemical approaches and advances towards the detection of drug resistance. *J Electrochem Soc.* 2020;167(4):045501.
- [6] Santoso HT. Electrochemical processing of polythiophene films with enhanced structural order [thesis]. Atlanta (GA): Georgia Institute of Technology; 2011.
- [7] Zhao Y, Nakanishi S, Watanabe K, et al. Hydroxylated and aminated polyaniline nanowire networks for improving anode performance in microbial fuel cells. *J Biosci Bioeng.* 2011;112(1):63–63.
- [8] Bleda-Martínez MJ, Peng C, Zhang S, et al. Electrochemical methods to enhance the capacitance in activated carbon/polyaniline composites. *J Electrochem Soc.* 2008;155(9): A672.
- [9] Gupta R, Singhal M, Nataraj SK, et al. A potentiostatic approach of growing polyaniline nanofibers in fractal morphology by interfacial electropolymerization. *RSC Adv.* 2016; 6(111):110416–110421.

- [10] Heinze J, Frontana-Urbe BA, Ludwigs S. Electrochemistry of conducting polymers-persistent models and new concepts. *Chem Rev.* 2010;110(8):4724–4771.
- [11] Schuhmann, W.; Kranz, C.; Wohlschläger, H, et al. Pulse technique for the electrochemical deposition of polymer films on electrode surfaces. *Biosens Bioelectron.* 1997; 12:1157–1167. doi:[https://doi.org/10.1016/S0956-5663\(97\)00086-9](https://doi.org/10.1016/S0956-5663(97)00086-9).
- [12] Duić LJ, Mandić Z, Kovačiček F. The effect of supporting electrolyte on the electrochemical synthesis, morphology, and conductivity of polyaniline. *J Polym Sci A Polym Chem.* 1994;32(1):105–111.
- [13] Imanishi K, Satoh M, Yasuda Y, et al. Solvent effect on electrochemical polymerization of aromatic compounds. *J Electroanal Chem Interfacial Electrochem.* 1988;242(1–2): 203–208. doi:(88)80251-1.
- [14] Okamoto H, Kotaka T. Structure and properties of polyaniline films prepared via electrochemical polymerization. I: effect of pH in electrochemical polymerization media on the primary structure and acid dissociation constant of product polyaniline films. *Polymer.* 1998;39(18):4349–4358.
- [15] Coelho MKL, Giarola JDF, Da Silva ATM, et al. Development and application of electrochemical sensor based on molecularly imprinted polymer and carbon nanotubes for the determination of carvedilol. *Chemosensors.* 2016;4(4):22.
- [16] Aslam J, Lone IH, Radwan N, et al. Development of poly (aniline-co-o-toluidine)/TiO₂ nanocomposite coatings for low carbon steel corrosion in 3.5% NaCl solution. *J Adhes Sci Technol.* 2018;32:2552–2568.
- [17] Abd El-Lateef HM, Alnajjar AO. Enhanced the protection capacity of poly (o-toluidine) by synergism with zinc or lanthanum additives at C-steel/HCl interface: a combined DFT, molecular dynamic simulations and experimental methods. *J Mol Liq.* 2020;303: 112641.
- [18] Jeyaprabha C, Sathiyarayanan S, Phani K, et al. Influence of poly (aminoquinone) on corrosion inhibition of iron in acid media. *Appl Surf Sci.* 2005;252(4):966–975.
- [19] Jeyaprabha C, Sathiyarayanan S, Phani K, et al. Investigation of the inhibitive effect of poly (diphenylamine) on corrosion of iron in 0.5 M H₂SO₄ solutions. *J Electroanal Chem Interfacial Electrochem.* 2005;585(2):250–255.
- [20] Sathiyarayanan S, Dhawan S, Trivedi D, et al. Soluble conducting poly ethoxy aniline as an inhibitor for iron in HCl. *Corros Sci.* 1992;33(12):1831–1841.
- [21] Yazdanpanah A, Ramedani A, Abrishamkar A, et al. Synthetic route of PANI (V): electrochemical polymerization. In: *Fundamentals and emerging applications of polyaniline.* Elsevier; 2019; 105–119. <https://doi.org/10.1016/B978-0-12-817915-4.00006-3>.
- [22] El Aggadi S, Loudiyi N, Chadil A, et al. Electropolymerization of aniline monomer and effects of synthesis conditions on the characteristics of synthesized polyaniline thin films. *MediterrJChem.* 2020;10(2):138–145.
- [23] Fang FF, Dong Y-Z, Choi HJ. Effect of oxidants on morphology of interfacial polymerized polyaniline nanofibers and their electrorheological response. *Polymer.* 2018;158: 176–182.
- [24] Gutic S, Cacan M, Korac F. Electrodeposition of polyaniline films on stainless steel and their voltammetric behavior in corrosive environments. *Bull Chem Technol Bosnia Herzegovina.* 2017; 48:45–50. doi:<https://www.researchgate.net/profile/Sanjin-Gutic/publication/322056790>.
- [25] Hui N, Chai F, Lin P, et al. Electrodeposited conducting polyaniline nanowire arrays aligned on carbon nanotubes network for high performance supercapacitors and sensors. *Electrochim Acta.* 2016;199:234–241.
- [26] Kaykha Y, Rafizadeh M. Template synthesis of fibrillar polyaniline complex using a degradable polyelectrolyte. *Mater Chem Phys.* 2019;229:98–105.
- [27] Umoren S, Obot I, Madhankumar A, et al. Technology. Effect of degree of hydrolysis of polyvinyl alcohol on the corrosion inhibition of steel: theoretical and experimental studies. *J Adhes Sci Technol.* 2015;29(4):271–295.

- [28] Solomon MM, Umoren S. Performance evaluation of poly (methacrylic acid) as corrosion inhibitor in the presence of iodide ions for mild steel in H₂SO₄ solution. *J Adhes Sci Technol*. 2015;29:1060–1080.
- [29] Tüken T, Arslan G, Yazıcı B, et al. The corrosion protection of mild steel by polypyrrole/polyphenol multilayer coating. *Corros Sci*. 2004;46(11):2743–2754.
- [30] Lakshmi D, Rajendran S, Sathiyabama J. Corrosion inhibition by phenols—an overview. *J Nano-Corrosion Sci Eng*. 2016;3:1–18.
- [31] Talati J, Modi RJCS. p-Substituted phenols as corrosion inhibitors for aluminium-copper alloy in sodium hydroxide. *Br Corros J*. 1979;19(1):35–48.
- [32] Aljeaban N, Goni L, Alharbi B, et al. Polymers decorated with functional motifs for mitigation of steel corrosion: an overview. *Int J Polym Sci*. 2020;2020:1–23.
- [33] Kassim MJ, Wei TK. Plants polyphenols: an alternative source for green corrosion inhibitor. In: *Proceedings of Proceedings of the Annual International Conference*. Syiah Kuala University-Life Sciences & Engineering Chapter. 2012; 2(2). <http://202.4.186.66/AICS-SciEng/article/view/1833>
- [34] Lai Y, Gao Y, Yao X, et al. Inhibition and adsorption behavior of thiophenol derivatives on copper corrosion in saline medium. *J Adhes Sci Technol*. 2021;1–20. <https://doi.org/10.1080/01694243.2021.1946306>
- [35] Xu H, Zhang Y. A review on conducting polymers and nanopolymer composite coatings for steel corrosion protection. *Coatings*. 2019;9(12):807.
- [36] Arpaia P, Buzio M, Capatina O, et al. Effects of temperature and mechanical strain on Ni-Fe alloy CRYOPHY for magnetic shields. *J Magn Magn Mater*. 2019;475:514–523.
- [37] Herrasti P, Recio F, Ocon P, et al. Effect of the polymer layers and bilayers on the corrosion behaviour of mild steel: comparison with polymers containing Zn microparticles. *Prog Org Coat*. 2005;54(4):285–291.
- [38] Hosseini M, Sabouri M, Shahrabi T. Corrosion protection of mild steel by polypyrrole phosphate composite coating. *Prog Org Coat*. 2007;60(3):178–185.
- [39] Trukhanov A, Grabchikov S, Solobai A, et al. AC and DC-shielding properties for the Ni₈₀Fe₂₀/Cu film structures. *J Magn Magn Mater*. 2017; 443:142–148.
- [40] Xie T, Fu L, Gao B, et al. The crystallization character of W-Cu thin films at the early stage of deposition. *Thin Solid Films*. 2019; 690:137555.
- [41] Zubar T, Sharko S, Tishkevich D, et al. Anomalies in Ni-Fe nanogranular films growth. *J Alloys Compd*. 2018; 748:970–978.
- [42] Ates M. A review on conducting polymer coatings for corrosion protection. *J Adhes Sci Technol* . 2016;30(14):1510–1536.
- [43] Ding Y, Zhong J, Xie P, et al. Protection of mild steel by waterborne epoxy coatings incorporation of polypyrrole nanowires/graphene nanocomposites. *Polymers*. 2019; 11: 1998.
- [44] Lee C, Lee YM, Moon MS, et al. UV-vis-NIR and raman spectroelectrochemical studies on viologen cation radicals: evidence for the presence of various types of aggregate species. *Electroanal Chem* . 1996;416(1-2):139–144. doi:(96)04741-9.
- [45] Manickavasagam R, Karthik KJ, Paramasivam M, et al. Poly (styrene sulphonic acid)-doped polyaniline as an inhibitor for the corrosion of mild steel in hydrochloric acid. *Anti-Corrosion Meth & Material*. 2002;49(1):19–26.
- [46] Abd El-Hafeez GM, El-Rabeie MM, Gaber AF, et al. Tailored polymer coatings as corrosion inhibitor for mild steel in acid medium. *J Coat Technol Res*. 2021;18(2): 581–590.
- [47] Pawar P, Sainkar S, Patil P. Synthesis of poly (aniline-co-o-toluidine) coatings and their corrosion-protection performance on low-carbon steel. *J Appl Polym Sci*. 2007;103(3): 1868–1878.
- [48] Badawy W, Al-Kharafi F, El-Azab A. Electrochemical behaviour and corrosion inhibition of Al, Al-6061 and Al-Cu in neutral aqueous solutions. *Corros Sci*. 1999;41(4): 709–727. doi:(98)00145-0.

- [49] Diggle J, Downie T, Goulding C. The dissolution of porous oxide films on aluminium. *Electrochim Acta* . 1970;15(7):1079–1093.
- [50] Ismail KM, El-Moneim AA, Badawy WA. Stability of Sputter-Deposited amorphous Mn-Ta alloys in Chloride-Free and Chloride-Containing H₂SO₄ solutions. *J Electrochem Soc*. 2001;148(2):C81–C87.
- [51] Arslan G, Yazici B, Erbil M. The effect of pH, temperature and concentration on electrooxidation of phenol. *J Hazard Mater*. 2005;124(1-3):37–43.
- [52] Gattrell M, Kirk D. A study of electrode passivation during aqueous phenol electrolysis. *J Electrochem Soc*. 1993;140(4):903–911.
- [53] Buzarovska A, Arsova I, Arsov L. Electrochemical synthesis of poly (2-methyl aniline): electrochemical and spectroscopic characterization. *J Serb Chem Soc*. 2001;66(1):27–37.
- [54] Sayyah S, El-Salam HM. Aqueous oxidative chemical polymerization of N-methylaniline in acid medium and characterization of the obtained polymer. *Int J Polym Mater*. 2003; 52:1087–1111.
- [55] Wei D, Kvarnström C, Lindfors T, et al. Electropolymerization mechanism of N-methylaniline. *Synthetic Metals*. 2006;156:541–548.
- [56] Hajjaji N, Rico I, Srhiri A, et al. Effect of N-alkylbetaines on the corrosion of iron in 1 M HCl solution. *Corrosion*. 1993;49(4):326–334.
- [57] Popova A, Sokolova E, Raicheva S. Relationship between the molecular structure of organic inhibitors and their protective action. II. Inhibitors in acidic media. *Khim Ind*. 1988;60:72–76.
- [58] Damaskin BB, Petrii OA, Batrakov VV. Adsorption of organic compounds on electrodes. New York: Plenum; 1971.